Superfluidity

E. V. Thuneberg

QTF Centre of Excellence, Department of Applied Physics, Aalto University, FI-00076 Aalto, Finland

Abstract

This chapter gives an introduction to basic properties of superfluids. After defining the subject, we list systems where it occurs: liquid ^{4}He, liquid ^{3}He, dilute atomic gases, neutron stars and superconducting metals. The microscopic basis for the formation of the superfluid phase is considered in boson and fermion systems. The two-fluid model is introduced and some consequences are discussed. The quantization of circulation is presented. Quantized vortex lines are introduced and they are used to explain the structure of a rotating superfluid. Phase slip, Josephson effect and critical velocity are discussed.

Keywords: Bose-Einstein condensation, counterflow, critical velocity, helium, Josephson effect, macroscopic wave function, quantized circulation, phase slip, second sound, order parameter, persistent current, superconductivity, superfluidity, two-fluid model, vortex line

- Definition of superfluidity
- Occurrence of superfluidity
- Microscopic basis of superfluidity
- Two-fluid model
- Quantized circulation, vortices and rotating superfluid
- Phase slip, Josephson effect and critical velocity

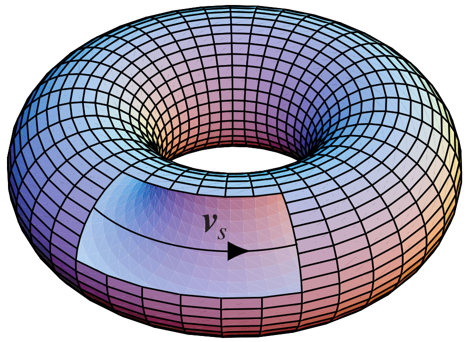

Figure 1: Once generated, the circulation of a superfluid (with velocity $\boldsymbol{v}_s$) persists as long as the experiment can be continued.

1. Introduction

Fluids (gases and liquids) are distinguished from solids by the property that they can flow. In almost all cases there is viscosity associated with the flow. Due to viscosity, the flow energy is gradually dissipated into heat. Contrary to this common situation, there is a special class of fluids, which can flow without viscosity. These are called *superfluids* and the phenomenon is called *superfluidity* (London, 1954; Tilley and Tilley, 1990; Guénault, 2003; Annett, 2004; Leggett, 2006; Bennemann and Ketterson, 2013; Barenghi and Parker, 2016). As a concrete example, consider a ring-shaped container filled with superfluid, see Fig. 1. Once the fluid is put into circular motion, it will continue to circulate and no energy is dissipated. The flow can continue as long as the external conditions remain unchanged, in particular the temperature is kept low enough.

Superfluids show many spectacular phenomena, which are discussed in sections 4-7. Before going into these we discuss the systems where superfluidity occurs (Sec. 2) and the microscopic basis of superfluidity (Sec. 3). While Sec. 3 gives deeper insight, it is not absolutely necessary for discussing the phenomena in Secs. 4-7.

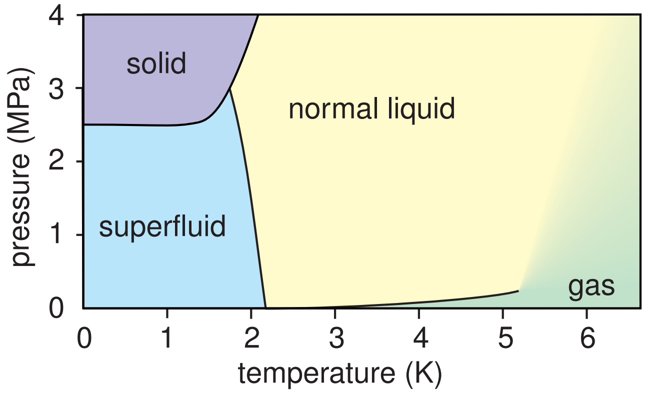

Figure 2: Phase diagram of ^{4}He at low temperatures. ^{4}He remains liquid at zero temperature if the pressure is below 2.5 MPa (approximately 25 atmospheres). The liquid has a phase transition to a superfluid phase, also known as He-II, at the temperature of 2.17 K (at vapor pressure).

2. Occurrence

Superfluidity occurs only in certain substances under special conditions. Superfluidity occurs at temperatures T below a transition temperature T_c, which strongly depends on the substance.

As a first case we discuss liquid helium. Under standard pressure and temperature helium is a gas. It liquifies at temperatures around 4 kelvin. Cooling further down, it enters the *superfluid phase* at temperatures around 2 kelvin, depending on pressure (Wilks, 1967). The phase diagram of natural helium at low temperatures is shown in Fig. 2. Natural helium consists essentially of isotope ^{4}He. A ^{4}He atom is a *boson* since both the electronic spin and the nuclear spin vanish. Helium was first liquefied in 1908 and the superfluid phase was discovered in 1938.

Helium has another stable isotope, ^{3}He. A ^{3}He atom is a *fermion* because the nuclear spin is 1/2. At temperatures below a few kelvin, its behavior is radically different from the isotope ^{4}He. It also becomes superfluid, but at temperatures that are a factor of one thousand smaller than for ^{4}He (Wheatley, 1975; Leggett,

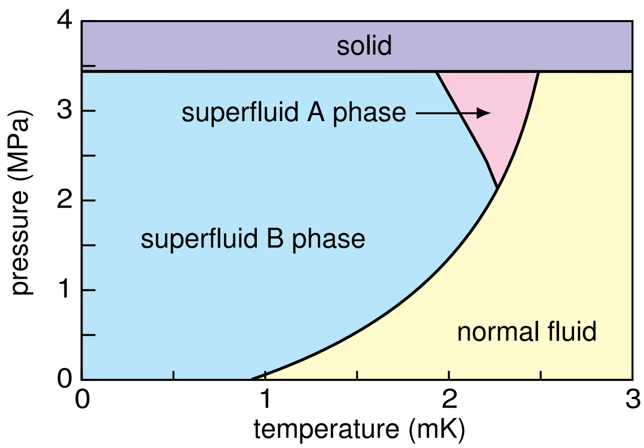

Figure 3: The phase diagram of ^{3}He at low temperatures. Note that the temperature is in units of millikelvin, in contrast to Fig. 2. Two superfluid phases, A and B, are shown. The figure is based on data by Greywall (1986).

1975; Vollhardt and Wölfle, 1990; Dobbs, 2001). The phase diagram of ^{3}He at low temperatures is shown in Fig. 3. ^{3}He has three different superfluid phases, A, A_1, and B. The A_1 phase only appears in magnetic field, and therefore is not visible in Fig. 3. Recently, also the polar phase has been demonstrated by adding dilute impurity, aerogel, into the liquid (Dmitriev et al., 2015). The superfluid phases A and B of ^{3}He were found in 1972.

With laser cooling it is possible cool certain dilute atomic gases like ^{1}H, ^{6}Li, ^{7}Li, ^{23}Na, ^{40}Ka, ^{87}Rb to very low temperatures. These gases condense to superfluid state at temperatures on the order of 1 μK, depending on the density and on atomic interactions (Pethick and Smith, 2002; Pitaevskii and Stringari, 2003; Leggett, 2006; Bloch et al., 2008). This state shows many properties that are similar to the helium superfluids, although it is not a thermodynamically stable state, and therefore the flow cannot last for ever. Most of the discussion in this article applies also to condensed gases. An important difference is that instead of container walls for helium liquids, one has to consider the confining potential of the gas, which can be generated either magnetically (by field gradients) or optically (by laser beams). The gas atoms ^{1}H, ^{7}Li, ^{23}Na, ^{87}Rb are bosons while ^{6}Li and ^{40}Ka are fermions. Superfluid condensation in a gas was first found in ^{87}Rb in 1995.

Superfluidity is expected to occur also in astrophysical objects. The neutron liquid in a neutron star is believed to be in a superfluid state (Page et al., 2014; Gezerlis et al., 2014; Chamel, 2017). Also protons in a neutron star are expected to condense to a superfluid state. Both neutrons and protons are fermions. The superfluidity has been suggested as an explanation for the observed sudden changes in the rotation velocity of pulsars.

Superfluidity is closely related to *superconductivity* (Tinkham, 1996; Bennemann and Ketterson, 2008). Superconductivity means that electric current can flow without resistance. This phenomenon appears in several elemental metals like Al, Sn, and Nb at temperatures on the order of 10 K or below. It also appears in several alloys and compounds. Superconductivity arises from resistanceless motion of the conduction electrons in a metal. Therefore, superconductivity can be understood as superfluidity of the conduction electrons, which are fermions. Part of the discussion in this article applies also to superconductivity, but there are differences caused mainly by two reasons. (a) Electrons have electric charge and therefore their motion is essentially coupled with magnetic field. (b) The crystal lattice of the ions constitutes a preferred frame of reference, which does not exist for helium liquids. Superconductivity was first found in Mercury in 1911.

3. Microscopic origin

In short, superfluidity can be explained as a quantum mechanical effect that shows up on a macroscopic scale.

Quantum mechanics is crucial in understanding the microscopic world. It explains that electrons in atoms have only discrete energies. There is no friction on the atomic scale, and the electrons can circulate the nucleus without losing energy.

We know that quantum mechanics rarely shows up on macroscopic scale. Instead of quantum mechanics, macroscopic objects obey the rules of classical physics. The reason is that a macroscopic sample consists of large number of particles and, instead of individual particles, one can only observe their average behavior. Usually the particles are in different quantum states, and an average over them obeys classical laws of physics. Examples of these laws are the Navier-Stokes equations for fluids and Ohm's law for electrical conduction.

Superfluidity is an exception to this general rule. In superfluids a macroscopic number of particles is in the same quantum state. It follows that summing over particles does not lead to averaging, but produces a *macroscopic wave function*.

Consider a free particle with mass m and momentum $\boldsymbol{p}$. Its kinetic energy is $E = p^2/2m$. Its state is represented by the single-particle wave function

$$\psi(\boldsymbol{r}) = \frac{1}{\sqrt{V}} \exp(\frac{i}{\hbar}\boldsymbol{p}\cdot\boldsymbol{r}), \tag{1}$$

where V is the volume of the system and $h = 2\pi\hbar$ the Planck constant. Below we also use the wave vector $\boldsymbol{k}$ so that $\boldsymbol{p} = \hbar\boldsymbol{k}$. The wave function of a many-body system $\Psi(\boldsymbol{r}_1, \boldsymbol{r}_2, \ldots)$ is more general and depends on the coordinates $\boldsymbol{r}_i$ of all particles, $i = 1, 2, \ldots, N$, where N is the number of particles.

Further analysis depends essentially whether the particles are bosons or fermions. We now assume the particles are bosons. This means that the total wave function must be symmetric when exchanging any pair of particles. In the case of two particles this means $\Psi(\boldsymbol{r}_1, \boldsymbol{r}_2) = \Psi(\boldsymbol{r}_2, \boldsymbol{r}_1)$. Further we assume that there is no interaction between the bosons. It can be shown that the occupation of the lowest energy state becomes macroscopic, if the temperature T is less than

$$T_{\mathrm{BE}} = \frac{h^2}{2\pi m k_B}\left(\frac{N}{2.612V}\right)^{2/3}. \tag{2}$$

Here k_B the Boltzmann constant. This is known as *Bose-Einstein condensation* (BEC). The wave function (1) of the lowest energy state ($\boldsymbol{p} = 0$) becomes macroscopic. At zero temperature, all particles are in this state.

While the ideal gas model explains Bose-Einstein condensation, it is quite insufficient in other respects. The interactions between particles are essential for the system to show superfluidity (see Sec. 7). In interacting system the macroscopically occupied state $\psi(\boldsymbol{r})$ need not be the lowest energy state, and thus the macroscopic wave function can be nontrivial. In Bose gases (^{87}Rb etc.) the interactions are weak, and a quantitative description can be achieved by the relatively simple Gross-Pitaevskii equation. In liquid ^{4}He the interactions are much stronger, and a quantitative theory is not easily achieved. But even in that case, formula (2) gives 3.1 K, which is not too far from the measured value. A simple phenomenological description of ^{4}He superfluid is obtained by considering its elementary excitations, see Fig. 4(a). The excitation spectrum is liner, $E(p) = cp$ at small momenta, where c is the velocity of sound. These excitations are known as phonons. At larger momenta $E(p)$ starts to decrease and it attains a minimum. The excitations near this minimum are known as rotons. In Bose gases only phonon excitations are visible because of weaker interactions.

Let us now turn to fermions. The fermions have spin, which has to be described by an additional index σ. Here we consider only spin-half particles, where the spin projection σ takes two values, $\sigma = \pm\frac{1}{2}$. The wave function of a fermion system is $\Psi(\boldsymbol{r}_1, \sigma_1, \boldsymbol{r}_2, \sigma_2, \ldots)$, and it has to be antisymmetric in the exchange of any pair of particles. For a two-particle state this means

$$\Psi(\boldsymbol{r}_1, \sigma_1, \boldsymbol{r}_2, \sigma_2) = -\Psi(\boldsymbol{r}_2, \sigma_2, \boldsymbol{r}_1, \sigma_1). \tag{3}$$

This implies that the occupation of any single-particle state only can be zero or one. This is known as the *Pauli exclusion principle*. Thus macroscopic occupation of a single-particle state (1) is not possible.

Superfluidity in a fermion system can appear as a result of an attractive interaction between particles. Such an interaction can cause formation of pairs. Each pair has to satisfy the antisymmetry condition (3). However, a pair is a unit that behaves like a boson. In particular, it is not excluded that several pairs are in the same pair state. Superfluidity in fermion systems can be understood

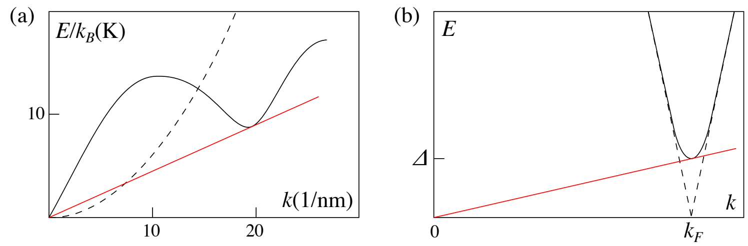

Figure 4: The energy of elementary excitations as a function of the wave number, $E(k)$. (a) Elementary excitations in liquid ^{4}He at vapor pressure (black solid line). The free atom kinetic energy is given by dashed line. The figure is based on neutron-scattering data by Henshaw and Woods (1961). (b) Sketch of elementary excitations of a degenerate fermion system. The excitation energy in the normal state (dashed lines) vanishes at the Fermi surface, $k = k_F$. The excitations are particle type at $k > k_F$ and hole type at $k < k_F$. In the superfluid state (black solid line) an energy gap Δ opens up. For visibility of the figure, the scales are far off from those ones in superconducting metals and liquid ^{3}He. In both panels the sloped straight lines (red) correspond the critical velocity according to Landau criterion (17).

as a macroscopic occupation of a single pair state. Thus superfluidity can be understood as Bose condensation of pairs.

The spin part of the pair wave function has four different possibilities. These can be classified as a singlet state

$$\uparrow\downarrow - \downarrow\uparrow \tag{4}$$

(which is a compact notation for $\delta_{\sigma_1,1/2}\delta_{\sigma_2,-1/2} - \delta_{\sigma_1,-1/2}\delta_{\sigma_2,1/2}$) and three triplet states, which can be chosen as

$$-\uparrow\uparrow + \downarrow\downarrow,\ i(\uparrow\uparrow + \downarrow\downarrow),\ \uparrow\downarrow + \downarrow\uparrow\,. \tag{5}$$

Let us first study the case of spin singlet (4). The pair wave function in this case is assumed to be of the form

$$\Psi(\boldsymbol{r}_1, \sigma_1, \boldsymbol{r}_2, \sigma_2) = \psi(\frac{\boldsymbol{r}_1 + \boldsymbol{r}_2}{2})\chi(\boldsymbol{r}_1 - \boldsymbol{r}_2)(\uparrow\downarrow - \downarrow\uparrow) \tag{6}$$

where we have separated the orbital wave function to a center of mass part ψ and a relative part χ. The singlet spin state (4) is antisymmetric in the exchange of the two spins. In order to satisfy pair antisymmetry (3), the corresponding orbital part $\chi(\boldsymbol{r}_1 - \boldsymbol{r}_2)$ has to be symmetric, $\chi(\boldsymbol{r}) = \chi(-\boldsymbol{r})$. In most superconductors the pair wave function is of the form (6). In majority of them (Al, Sn, Nb, ...) χ is approximately independent of the direction of $\boldsymbol{r}_1 - \boldsymbol{r}_2$. This is called s-wave pairing in analogy with s, p, d, etc. atomic orbitals. In high-T_c superconductors there is strong evidence of d-wave symmetry of χ. In Fermi gases s-wave pairing has been observed with the spin being pseudo spin formed by two atomic hyperfine states. (Zwierlein, 2014).

Another alternative is that the spin state of a pair is triplet (5). This case is realized in ^{3}He and possibly in some superconductors. In ^{3}He the orbital wave function is of p type. There are three degenerate p-wave states p_x, p_y and p_z. The pair wave function can be written as

$$\Psi(\boldsymbol{r}_1, \sigma_1, \boldsymbol{r}_2, \sigma_2) = \sum_{j=1}^{3} \sum_{\mu=1}^{3} \psi_{\mu j}(\frac{\boldsymbol{r}_1 + \boldsymbol{r}_2}{2}) p_j(\boldsymbol{r}_1 - \boldsymbol{r}_2) i\hat{\sigma}_\mu \hat{\sigma}_2. \tag{7}$$

Here $i\hat{\sigma}_\mu \hat{\sigma}_2$ denotes the same three spin states as in Eq. (5), but expressed using Pauli spin matrices $\hat{\sigma}_i$.

The macroscopic wave function of bosons is called *order parameter*, since it describes ordering of the particles and it vanishes in the normal fluid phase. For fermions the same role is played by the center of mass part of the pair function. This is the soft degree of freedom, which can change as a function of time and location, whereas the other parts in the pair wave function (6)-(7) are fixed. We see that the order parameter in ^{4}He and in most superconductors is a complex-valued scalar ψ, but in ^{3}He it is a 3×3 matrix $\psi_{\mu j}$. The order parameter in condensed boson gases is a scalar in the simplest case, but including atoms in different hyperfine states allows more complicated forms. In neutron stars both spin singlet and triplet pairing has been predicted to occur.

An important energy scale in a Fermi system is *Fermi energy*. It is the energy up to which all noninteracting single particle states would be filled at zero temperature. It is $E_F = p_F^2/2m$, where the Fermi momentum p_F is related to the particle density by $N/V = p_F^3/3\pi^2\hbar^3$. Compared with thermal energy $k_B T$, it corresponds to Fermi temperature $T_F = E_F/k_B$. For ^{3}He $T_F \sim 1$

K and for elemental superconductors $T_F \sim 10^4$ K. We see that for both ^{3}He and superconductors, the transition temperature is small compared to the Fermi temperature, $T_c/T_F \sim 10^{-3}$ or less. This implies that only excitations that have low energy ($\ll E_F$) close to the Fermi surface $p = p_F$ play role in superfluidity. Such excitations are described by Landau's *Fermi liquid theory*. The normal state excitations are quasiparticles which are free-particle like and weakly interacting, see Fig. 4(b). In the superfluid state pairs are formed. They are weakly bound and called Cooper pairs. The pair condensation opens an energy gap in the excitation spectrum. Quantitative theory of fermion superfluids is based on the Bardeen-Cooper-Schrieffer (BCS) theory of superconductivity (Bardeen et al., 1957). The extension to cover superfluid ^{3}He is discussed by Serene and Rainer (1983).

Above we have discussed the boson and fermion cases separately. But in fact, one can think to go continuously from one case to the other. By increasing the attractive interaction of the fermions in a Cooper pair, one could transform it to a strongly bound pair, which could be considered as a single Bose particle. This BCS-BEC crossover has been experimentally studied in fermion gases.

4. Hydrodynamics

Many properties of superfluids can be understood in terms of the *two-fluid model*. The basic assumption is that the liquid consists of two parts. These are called the *superfluid* and *normal components*. The current density $\boldsymbol{j}$ can be represented as a sum

$$\boldsymbol{j} = \rho_s \boldsymbol{v}_s + \rho_n \boldsymbol{v}_n. \tag{8}$$

Here ρ_s and $\boldsymbol{v}_s$ are the density and velocity of the superfluid component and ρ_n and $\boldsymbol{v}_n$ are the corresponding quantities for the normal component. The liquid density is the sum of the two densities, $\rho = \rho_s + \rho_n$. The superfluid component can flow without viscosity and it carries no heat or entropy. Moreover it is curl free,

$$\boldsymbol{\nabla} \times \boldsymbol{v}_s = 0. \tag{9}$$

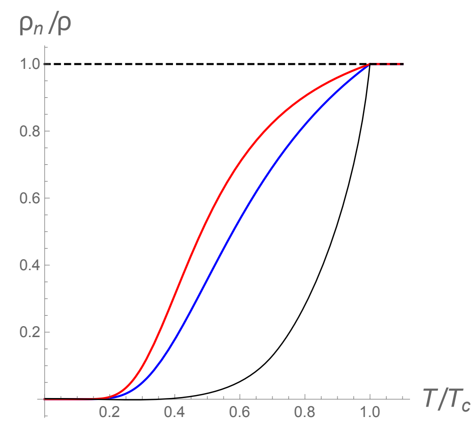

Figure 5: The normal fluid fraction ρ_n/ρ as a function of temperature relative to T_c. The lowest curve is for superfluid ^{4}He at vapor pressure and is based on data in Peshkov (1946). The other curves are for superfluid ^{3}He-B at melting pressure (upper curve) and vapor pressure (middle curve) according to weak coupling theory (BCS theory generalized to triplet p-pairing and including Fermi-liquid interactions). The superfluid fraction $\rho_s/\rho = 1 - \rho_n/\rho$.

(This is valid only in uncharged superfluids.) The normal component behaves more like a usual viscous fluid.

The two-fluid model can be justified from the microscopic theory discussed in Sec. 3. The superfluid component corresponds to particles in the macroscopic wave function, and the normal component to particles in the excited states. The densities of the two components depend on temperature. At zero temperature all particles are in the condensate, $\rho_n = 0$ and $\rho_s = \rho$. With increasing temperature more particles are excited out of the condensate to the excited states. Thus $\rho_n(T)$ grows and $\rho_s(T)$ drops, see Fig. 5. The superfluid transition T_c is the temperature at which the condensate ceases to exist, and corresponds to $\rho_s = 0$ and $\rho_n = \rho$.

In application of the two-fluid model we can distinguish two cases. Consider first the case that only the superfluid component moves, $v_n = 0$. This can be realized in the ring-shaped container (Fig. 1). Once the superfluid component is set into motion, it can persists because flow is ideal with no viscosity. This

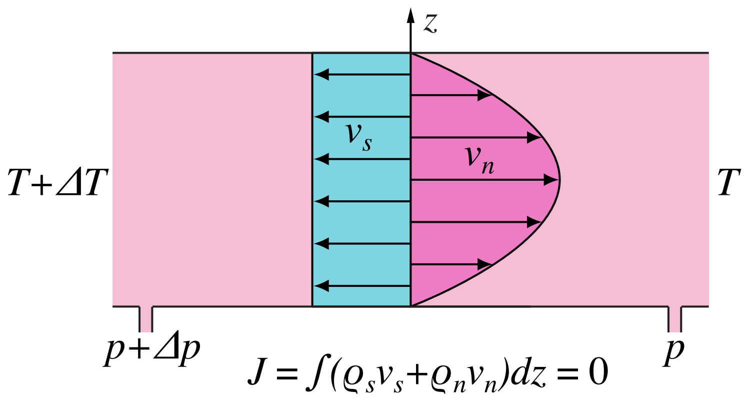

Figure 6: A difference in temperature ΔT generates flow of normal and superfluid components in opposite directions, and a pressure difference Δp appears. The viscosity of the normal component causes v_n to vanish at walls. The superfluid velocity $v_s(z)$ has to be constant in order to be curl free (9). In a channel with closed ends the total mass flow J has to vanish.

explains that superfluid can flow through narrow pores or as a thin film in response to small or vanishing pressure difference.

The other type of motion is that also the normal component participates in it. This takes place, for example, when an object moves in the liquid. Because of motion of the normal component, viscous forces and dissipation appear. This explains that nonvanishing viscosity is measured with a viscometer, where the superfluid is placed between two plates or coaxial cylinders that move at different velocities. The measured viscosity can still be small at low temperatures, where the normal component density is vanishingly small.

Superfluids show peculiar mixing of thermal and mechanical properties. Consider superfluid in a channel which is heated at one end, see Fig. 6. The superfluid component is attracted to the hot region because the chemical potential is lower there. As a consequence a pressure difference appears. This drives the normal component in the direction of decreasing temperature and convects the heat away from the source. Assuming the geometry does not allow net mass transfer, the mass transported by the normal and superfluid components in opposite directions are equal in magnitude. Such *counterflow* can lead to exceptionally large heat conductance.

In addition to usual sound wave, superfluids have another propagating mode. This *second sound* is an oscillation where normal and superfluid components move in opposite directions. This leads to oscillation of temperature whereas the density remains nearly constant. Second sound can be generated by heating the superfluid periodically, and standing waves of temperature have been demonstrated experimentally.

In addition to the mass current $\boldsymbol{j}$, there can be persistent spin currents. This is possible in superfluids whose order parameter is more complicated than scalar (^{3}He). Spin current is described by a tensor $j_{\mu j}^{\rm spin}$. The index $\mu = x, y, z$ indicates the direction of spin angular momentum that is flowing, and $j = x, y, z$ indicates the direction of the flow. Even in equilibrium the order parameter of ^{3}He has nontrivial spatial variation called *texture*. This is associated with persistent spin currents and, in case of ^{3}He-A, also with persistent mass currents.

5. Quantization of circulation

Consider a superfluid with order parameter ψ. (Assume an uncharged superfluid, ψ can be either scalar or matrix.) The superfluid velocity $\boldsymbol{v}_s$ can be expressed as a function of the order parameter as

$$\boldsymbol{v}_s = \frac{\hbar}{M} \boldsymbol{\nabla} \phi. \tag{10}$$

Here $\phi(\boldsymbol{r})$ is the phase of the order parameter, $\psi(\boldsymbol{r}) = A e^{i\phi(\boldsymbol{r})}$, and the amplitude A is assumed constant. M is the boson mass, i.e. the mass of a particle in a boson superfluid and the mass of a pair in a fermion superfluid. Eq. (10) can be justified starting from the expression of current in quantum mechanics.

An alternative form of Eq. (10) is obtained by taking line integral along a closed path,

$$\oint \boldsymbol{v}_s \cdot d\boldsymbol{l} = N \frac{h}{M}. \tag{11}$$

Here we have used the property that ϕ is defined modulo 2π, and N is an integer. Eq. (11) is known as *quantization of circulation*. The curl-free condition (9) is a direct consequence of Eq. (10) or (11).

Consider again superfluid in a ring-shaped container (Fig. 1). We can apply Eq. (11) to a path in the ring. We see that, in addition to being persistent, the superfluid velocity can only have discrete values. A similar phenomenon in superconductors is *flux quantization*. It says that magnetic flux through a ring shaped superconductor is an integral multiple of flux quantum $\Phi_0 = h/2e$, where e is the elementary charge.

6. Rotating superfluid and vortex lines

Let us consider superfluid in a container that is rotated with angular velocity $\boldsymbol{\Omega}$. The normal component will follow this motion because of its viscosity. In equilibrium it rotates uniformly with the container, $\boldsymbol{v}_n = \boldsymbol{\Omega} \times \boldsymbol{r}$. This is not possible for the superfluid component because it has to be curl free (9). [Eq. (9) should be compared to $\boldsymbol{\nabla} \times \boldsymbol{v}_n = 2\boldsymbol{\Omega}$.]

The rotating state of a superfluid is most commonly realized by *vortex lines* (Andronikashvili and Mamaladze, 1966; Donnelly, 1991). On a path around the vortex line, the phase ϕ changes by 2π (or an integral multiple of it). This is illustrated in Fig. 7. Equivalently, the circulation of superfluid velocity (11) around the vortex line is h/M. Assuming cylindrical symmetry, the phase ϕ is the same as the azimuthal angle in the cylindrical coordinate system (r, ϕ, z). The velocity field can be calculated from Eq. (10):

$$\boldsymbol{v}_s = \frac{\hbar}{Mr}\hat{\boldsymbol{\phi}}, \tag{12}$$

where $\hat{\boldsymbol{\phi}}$ is a unit vector in the azimuthal direction.

The structure of the rotating state is determined by minimum of free energy. The rotation of the container is taken into account by minimizing $F = F_0 - \boldsymbol{L}\cdot\boldsymbol{\Omega}$, where F_0 is the free energy functional in the stationary case and $\boldsymbol{L}$ the angular

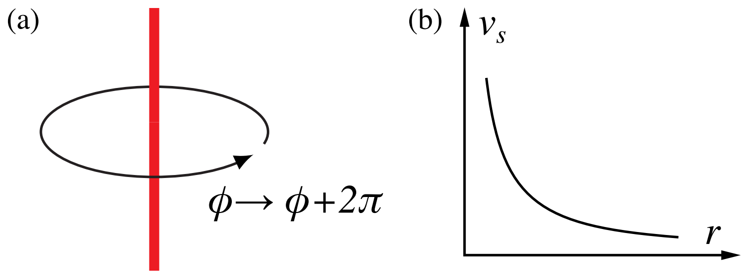

Figure 7: (a) Schema of a vortex line, where the phase of the order parameter changes by 2π when encircling the line. (b) Dependence of the azimuthal velocity field (12) on the distance r from the vortex line.

momentum. In the two-fluid model this reduces to

$$F = \int d^3r \frac{1}{2}\rho_s(\boldsymbol{v}_s - \boldsymbol{v}_n)^2 + \text{constant}. \quad (13)$$

Thus the optimal solution corresponds to $\boldsymbol{v}_s$ as equal as possible to $\boldsymbol{v}_n = \boldsymbol{\Omega} \times \boldsymbol{r}$, but subject to condition (10). This is achieved by a regular array of vortex lines, see Fig. 8. The number of vortex lines n per unit area is determined by the condition that the circulations of normal and superfluid velocities are the same over an area containing many vortex lines. This yields

$$n = \frac{2M\Omega}{h}. \quad (14)$$

There are approximately 1000 vortex lines in a circular container of radius 1 cm that is rotating 1 round per minute.

Vortex lines in an uncharged superfluid are analogous to *flux lines*, which occur in type II superconductors. Flux lines of superconductors appear in magnetic field, which is analogous to rotation of an uncharged superfluid.

The velocity field (12) of a vortex diverges at the vortex line. Thus there must be a *vortex core*, where the two-fluid description is insufficient. A finite energy in the vortex core is achieved if the amplitude of the order parameter vanishes at the vortex line. This is the case for a scalar order parameter. For a matrix order parameter it is not necessary that all components of the matrix vanish at the line. Such vortex lines are realized in superfluid ^{3}He-B.

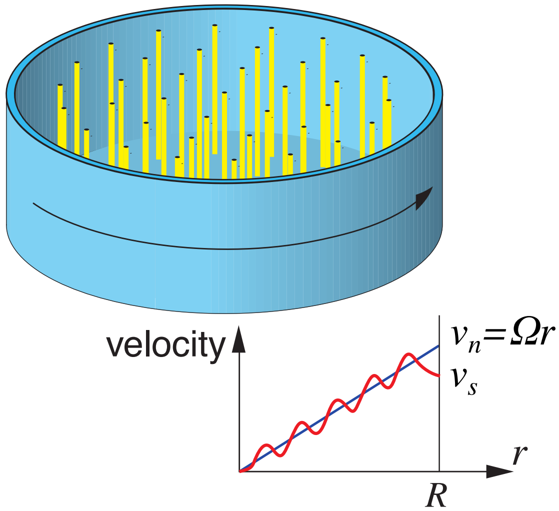

Figure 8: In a rotating container the vortex lines form a regular array so that the superfluid and normal fluid velocities, v_s and v_n, are equal on the average. In equilibrium the vortex array rotates rigidly with the container.

The quantization of the superfluid velocity (11) is not always true for uncharged superfluids. This happens when there is an additional contribution to the superfluid velocity (10) coming from the matrix form of the order parameter. Such a case is realized in superfluid ^{3}He-A, and careful reanalysis of the rotating state is needed. It turns out that, in addition to one-dimensional vortex lines, the vorticity may be arranged as two-dimensional vortex sheets and three-dimensional textures. All these have been confirmed experimentally (Lounasmaa and Thuneberg, 1999). In any case, a homogeneous rotation of the superfluid is excluded. Many more topological objects in quantum liquids and their parallels in particle physics and cosmology are discussed by Volovik (2003).

Besides rotating superfluid, vortex lines appear also in other circumstances. Vortices are important in limiting the maximal flow velocity, as will be discussed in the following section. By strong mechanical driving or by large thermal counterflow (Fig. 6) one can generate a large number of vortices. This is the quantum version of turbulence (Skrbek et al., 2021). In three dimensions the energy of vortex lines is high relative to the quasiparticle excitations, and therefore they are not important for thermodynamics. This changes in a thin liquid film, which forms essentially a 2 dimensional system. The transition from superfluid to normal state can be seen as formation of free vortices that destroy the superfluid coherence, which is known as Kosterlitz-Thouless transition.

7. Phase slip, Josephson effect and critical velocity

Let us study superflow in a channel under thermal equilibrium ($\boldsymbol{v}_n = 0$). The maximum supercurrent is determined by a process called *phase slip*. Consider that a short piece of vortex line is nucleated at a surface on one side of the channel. This vortex expands, goes through the whole cross section of the channel, and finally disappears on the other side. As a result of this process, the phase difference $\Delta\phi$ between the ends of the channel has changed by 2π. Part of the superfluid kinetic energy is dissipated in the motion of the vortex. This means that the flow ceases to be dissipationless above a critical velocity for phase slips. Phase slips preferentially take place in constrictions of the flow channel, where the superfluid velocity has its maximum value.

A special type of phase slip takes place in very short constrictions, where Eq. (10) ceases to be valid. An ideally short constriction shows the *Josephson effect*, where the supercurrent J_s depends on the phase difference $\Delta\phi$ as

$$J_s = J_c \sin(\Delta\phi), \tag{15}$$

and J_c is a constant. Moreover, the time derivative of $\Delta\phi$ is proportional to the difference of the chemical potential $\Delta\mu$ on the two sides of the constriction,

$$\frac{d\Delta\phi}{dt} = -\frac{2\Delta\mu}{\hbar}. \tag{16}$$

Combining the two equations, one sees that a constant $\Delta\mu$ generates an oscillating current at the frequency $2\Delta\mu/h$.

The Josephson effect takes place in all superfluids. It has extensively been studied in superconductors, where it is straightforward to fabricate barriers through which electrons can tunnel. For helium one has to use sufficiently small constrictions. Josephson effect in ^{3}He has been discussed by Davis and Packard (2002).

Let us consider a macroscopic moving object in a stationary superfluid. As discussed above, there generally is viscous drag from the normal component, but restricting to low temperatures, say below $0.2T_c$, the normal fraction is vanishingly small. In this case the motion is nearly dissipationless as long as the object does not generate new excitations. The creation of excitations is limited by energy and momentum conservation. A simple calculations shows that no excitations are generated below the velocity

$$v_c = \min \frac{E(p)}{p}, \tag{17}$$

which means the minimum of $E(p)/p$ over all excitations. In connection of superfluidity, the velocity (17) is known as Landau velocity. It is more general, however, because the condition $v < v_c = \min \omega(k)/k$ means relatively low dissipation in any system, where the medium has waves with angular frequency ω and wave number k. The critical velocity (17) can also be derived from the condition that the waves generated by the object are stationary in the frame where the object is at rest. This is familiar to us, for example, from waves generated by a ship on the surface of water.

When the object velocity exceeds the Landau velocity v_c, a steep increase of the drag force is expected. Let us examine this in special cases. For ^{4}He the critical velocity is determined by the roton minimum [sloped line in Fig. 4(a)]. This gives $v_c \approx 60$ m/s. Landau critical velocity has been observed for ions moving in superfluid ^{4}He under pressure. In most experiments, the measured critical velocity is much lower. This is commonly interpreted to be caused by vortices, which are hard to avoid in a macroscopic set up.

For ^{3}He-B the Landau velocity $v_c = \Delta/p_F$, which corresponds to 27 mm/s at vapor pressure. Again, critical velocity of this magnitude has been seen with moving ions. For macroscopic objects the measured critical velocity is smaller than this. However, a recent experiment observes very little dissipation up to velocity $\sim 2v_c$ (Bradley et al., 2016). At the time of writing, this is not understood theoretically (Kuorelahti et al., 2018).

Landau velocity has also been applied to cases where only the superfluid component is in motion. For example, in ideal boson gas and in normal state fermions (dashed lines in Fig. 4) it gives vanishing critical velocity, $v_c = 0$. This is consistent with other arguments that these systems are not superfluids. However, for non-s-wave pairing of fermions, it is possible that the energy gap Δ depends on the point on the Fermi surface, and can have nodes, leading to $v_c = 0$. Such a case appears ^{3}He-A. In this case the vanishing of the Landau velocity does not imply absence of superfluidity.

8. Conclusion

We have given introduction to the basic properties of superfluids. Several more advanced topics are mentioned, but all details of them are left to be read from the given references and other literature.

References

Andronikashvili, E.L., Mamaladze, Y.G., 1966. Quantization of macroscopic motions and hydrodynamics of rotating helium ii. Rev. Mod. Phys. 38, 567–625. URL: `https://link.aps.org/doi/10.1103/RevModPhys.38.567`, doi:`10.1103/RevModPhys.38.567`.

Annett, J.F., 2004. Superconductivity, Superfluids, and Condensates. Oxford, Oxford.

Bardeen, J., Cooper, L.N., Schrieffer, J.R., 1957. Theory of superconductivity. Phys. Rev. 108, 1175–1204. URL: `https://link.aps.org/doi/10.1103/PhysRev.108.1175`, doi:`10.1103/PhysRev.108.1175`.

Barenghi, C.F., Parker, N.G., 2016. A Primer on Quantum Fluids. Springer.

Bennemann, K.H., Ketterson, J.B. (Eds.), 2008. Superconductivity. volume I-II. Springer, Heidelberg.

Bennemann, K.H., Ketterson, J.B. (Eds.), 2013. Novel Superfluids. volume I. Oxford, Oxford.

Bloch, I., Dalibard, J., Zwerger, W., 2008. Many-body physics with ultracold gases. Rev. Mod. Phys. 80, 885–964. URL: https://link.aps.org/doi/10.1103/RevModPhys.80.885, doi:10.1103/RevModPhys.80.885.

Bradley, D.I., Fisher, S.N., Guénault, A.M., Haley, R.P., Lawson, C.R., Pickett, G.R., Schanen, R., Skyba, M., Tsepelin, V., Zmeev, D.E., 2016. Breaking the superfluid speed limit in a fermionic condensate. Nature Physics 12, 1017–1021. URL: https://doi.org/10.1038/nphys3813, doi:10.1038/nphys3813.

Chamel, N., 2017. Superfluidity and superconductivity in neutron stars. Journal of Astrophysics and Astronomy 38, 43. URL: https://doi.org/10.1007/s12036-017-9470-9, doi:10.1007/s12036-017-9470-9.

Davis, J.C., Packard, R.E., 2002. Superfluid ^{3}He josephson weak links. Rev. Mod. Phys. 74, 741–773. URL: https://link.aps.org/doi/10.1103/RevModPhys.74.741, doi:10.1103/RevModPhys.74.741.

Dmitriev, V.V., Senin, A.A., Soldatov, A.A., Yudin, A.N., 2015. Polar phase of superfluid ^{3}He in anisotropic aerogel. Phys. Rev. Lett. 115, 165304. URL: https://link.aps.org/doi/10.1103/PhysRevLett.115.165304, doi:10.1103/PhysRevLett.115.165304.

Dobbs, E.R., 2001. Helium Three. Oxford, Oxford.

Donnelly, R.J., 1991. Quantized Vortices in Helium II. Cambridge, Cambridge.

Gezerlis, A., Pethick, C.J., Schwenk, A., 2014. Pairing and superfluidity of nucleons in neutron stars, in: Bennemann, K.H., Ketterson, J.B. (Eds.), Novel Superfluids. Oxford, Oxford. volume 2. chapter 22, pp. 580–615.

Greywall, D.S., 1986. ^{3}He specific heat and thermometry at millikelvin temperatures. Phys. Rev. B 33, 7520–7538. URL: https://link.aps.org/doi/10.1103/PhysRevB.33.7520, doi:10.1103/PhysRevB.33.7520.

Guénault, T., 2003. Basic Superfluids. Taylor & Francis, London.

Henshaw, D.G., Woods, A.D.B., 1961. Modes of atomic motions in liquid helium by inelastic scattering of neutrons. Phys. Rev. 121, 1266–1274. URL: https://link.aps.org/doi/10.1103/PhysRev.121.1266, doi:10.1103/PhysRev.121.1266.

Kuorelahti, J.A., Laine, S.M., Thuneberg, E.V., 2018. Models for supercritical motion in a superfluid fermi liquid. Phys. Rev. B 98, 144512. URL: https://link.aps.org/doi/10.1103/PhysRevB.98.144512, doi:10.1103/PhysRevB.98.144512.

Leggett, A.J., 1975. A theoretical description of the new phases of liquid ^{3}He. Rev. Mod. Phys. 47, 331–414. URL: https://link.aps.org/doi/10.1103/RevModPhys.47.331, doi:10.1103/RevModPhys.47.331.

Leggett, A.J., 2006. Quantum Liquids: Bose Condensation and Cooper Pairing in Condensed-Matter Systems. Oxford, Oxford.

London, F., 1954. Superfluids, vol. II. Wiley, New York.

Lounasmaa, O.V., Thuneberg, E., 1999. Vortices in rotating superfluid 3he. Proceedings of the National Academy of Sciences 96, 7760–7767. URL: https://www.pnas.org/content/96/14/7760, doi:10.1073/pnas.96.14.7760, arXiv:https://www.pnas.org/content/96/14/7760.full.pdf.

Page, D., Lattimer, J.M., Prakash, M., Steiner, A.W., 2014. Stellar superfluids, in: Bennemann, K.H., Ketterson, J.B. (Eds.), Novel Superfluids. Oxford, Oxford. volume 2. chapter 21, pp. 505–579.

Peshkov, V.P., 1946. Determination of the velocity of propagation of the second sound in helium ii. Journal of Physics (Moscow) 10, 389.

Pethick, C.J., Smith, H., 2002. Bose–Einstein Condensation in Dilute Gases. Cambridge, Cambridge.

Pitaevskii, L., Stringari, S., 2003. Bose-Einstein condensation. Oxford, Oxford.

Serene, J., Rainer, D., 1983. The quasiclassical approach to superfluid 3he. Physics Reports 101, 221–311. URL: https://www.sciencedirect.com/science/article/pii/0370157383900510, doi:https://doi.org/10.1016/0370-1573(83)90051-0.

Skrbek, L., Schmoranzer, D., Midlik, Š., Sreenivasan, K.R., 2021. Phenomenology of quantum turbulence in superfluid helium. Proceedings of the National Academy of Sciences 118. URL: https://www.pnas.org/content/118/16/e2018406118, doi:10.1073/pnas.2018406118, arXiv:https://www.pnas.org/content/118/16/e2018406118.full.pdf.

Tilley, D.R., Tilley, J., 1990. Superfluids, vol. II. IOP publishing, Bristol.

Tinkham, M., 1996. Introduction to superconductivity. 2 ed., McGraw-Hill, New York.

Vollhardt, D., Wölfle, P., 1990. The superfluid phases of helium 3. Taylor & Francis, London.

Volovik, G.E., 2003. The Universe in a Helium Droplet. Clarendon, Oxford.

Wheatley, J.C., 1975. Experimental properties of superfluid ^{3}He. Rev. Mod. Phys. 47, 415–470. URL: https://link.aps.org/doi/10.1103/RevModPhys.47.415, doi:10.1103/RevModPhys.47.415.

Wilks, J., 1967. The properties of liquid and solid helium. Clarendon, Oxford.

Zwierlein, M.W., 2014. Superfluidity in ultracold atomic fermi gases, in: Bennemann, K.H., Ketterson, J.B. (Eds.), Novel Superfluids. Oxford, Oxford. volume 2. chapter 18, pp. 269–422.